Characterization of Pore Structure in a Nanoporous Low-Dielectric-Constant Thin Film by Neutron Porosimetry and X-ray Porosimetry

Ronald C. Hedden,* Hae-Jeong Lee, Christopher L. Soles, and Barry J. Bauer

Polymers Division, National Institute of Standards and Technology, Gaithersburg, Maryland 20899

Received December 10, 2003. In Final Form: May 21, 2004

A small-angle neutron scattering (SANS) porosimetry technique is presented for characterization of pore structure in nanoporous thin films. The technique is applied to characterize a spin-on organosilicate low dielectric constant (low-*k*) material with a random pore structure. Porosimetry experiments are conducted using a "contrast match" solvent (a mixture of toluene-d_8 and toluene-h_8) having the same neutron scattering length density as that of the nanoporous film matrix. The film is exposed to contrast match toluene vapor in a carrier gas (air), and pores fill with liquid by capillary condensation. The partial pressure of the solvent vapor is increased stepwise from 0 (pure air) to P_0 (saturated solvent vapor) and then decreased stepwise to 0 (pure air). As the solvent partial pressure increases, pores fill with liquid solvent progressively from smallest to largest. SANS measurements quantify the average size of the empty pores (those not filled with contrast match solvent). Analogous porosimetry experiments using specular X-ray reflectivity (SXR) quantify the volume fraction of solvent adsorbed at each step. Combining SXR and SANS data yields information about the pore size distribution and illustrates the size dependence of the filling process. For comparison, the pore size distribution is also calculated by application of the classical Kelvin equation to the SXR data.

Introduction

In recent years, the microelectronics industry has developed a wide variety of nanoporous thin films (low-*k* dielectrics) intended for use as electrical insulators for integrated circuits.[1] Hundreds of potential low-*k* materials containing <10−100 Å pores have been developed, including both organosilicates and organic polymer materials. Optimization of these new mesoporous low-*k* materials for applications requires thorough understanding of the way pore structure influences mechanical, thermal, and barrier properties. (Mesoporous materials are defined as those having a pore diameter of about 20−500 Å.[2] Measurement of low-*k* material structural characteristics such as pore volume fraction, morphology, size distribution, and connectivity, therefore, continues to be an important challenge.

In this report, we present a methodology for pore structure determination based on a new approach to *capillary porosimetry*. The science of capillary porosimetry uses vapor adsorption measurements to characterize pore size distribution (PSD). When a mesoporous material is exposed to a solvent vapor, liquid may condense in the pores. A vapor−liquid interface confined inside a very small pore will have a finite radius of curvature, and the saturated vapor pressure is reduced above the curved surface. When the material is exposed to solvent vapor at an external partial pressure P, pores fill with liquid if their dimensions are less than or equal to some critical minimum size r for which the saturated vapor pressure in the pore equals P. In the porosimetry experiment, the adsorption of the liquid in the porous material is measured as a function of external solvent partial pressure. Let P be the external partial pressure of the probe solvent and let P_0 be its saturated vapor pressure over a flat surface. The mass uptake or volume fraction of liquid due to adsorption is measured by a suitable analytical technique as the relative pressure P/P_0 is increased stepwise from 0 to 1 (adsorption) and then decreased stepwise to 0 (desorption). During adsorption, the smallest pores generally fill with solvent at low values of P/P_0, followed by filling of progressively larger pores as P/P_0 increases until all solvent-accessible pores are filled at $P/P_0 = 1$. Pore emptying during desorption generally occurs in reverse order from largest pores to smallest, although solvent uptake may exhibit a different dependence on P/P_0 as a result of issues associated with pore shape and connectivity. Characteristics of the PSD are inferred from the adsorption−desorption data usually by application of a physical model that relates the critical pore size r to P/P_0.

In the current study, a new approach, capillary porosimetry, is taken to characterize mesoporous thin films. As P/P_0 is varied, pore size is measured directly by in situ small-angle neutron scattering (SANS) instead of by applying a physical model. SANS porosimetry is conducted using a "contrast match" solvent having the same neutron scattering length density (SLD) as the matrix of the porous material. At any given value of P/P_0, any pores filled with the liquid solvent match the neutron SLD of the matrix. The coherent scattered intensity $I(q)$, therefore, largely arises from the contrast between the empty portion of pores (i.e., those not filled with solvent) and the matrix. By fitting SANS data at each value of P/P_0 to an appropriate model, an average pore size is measured that corresponds only to the portion of the pores not filled with solvent. Because the smallest pores fill with solvent at low values of P/P_0, followed by progressively larger pores as P/P_0 increases, the SANS measurement characterizes sub-populations of pores of increasing average size,

* Corresponding author. Present address: Dept. of Materials Science and Engineering, The Pennsylvania State University, University Park, PA 16802. E-mail: hedden@matse.psu.edu.

(1) Maex, K.; Baklanov, M. R.; Shamiryan, D.; Lacopi, F.; Brongersma, S. H.; Yanovitskaya, Z. S. *J. Appl. Phys.* **2003**, *93* (11), 8793−8841.

(2) Everett, D. H. Manual of Symbols and Terminology for Physicochemical Quantities and Units. *Pure Appl. Chem.* **1972**, *31*, 577−638 (Appendix II: Definitions, terminology and symbols in colloid and surface chemistry - part 1: Colloid and Surface Chemistry).

10.1021/la036334u
Published on Web 07/02/2004

probing different parts of the PSD. When all pores are filled, the coherent part of the scattered intensity drops to 0 over all q as the material becomes homogeneous in neutron SLD. If the volume fraction of liquid solvent ϕ_s is independently measured as a function of P/P_0, the dependence of the average pore size on ϕ_s more completely characterizes the PSD. The volume fraction of the solvent ϕ_s may be measured by an independent technique such as the X-ray reflectivity.

In this report, the SANS porosimetry technique is introduced and a spin-on polymethylsilsesquioxane (MSQ) low-k dielectric is characterized to illustrate the methodology. To more completely characterize the pore-filling process, complementary measurements of solvent uptake ϕ_s versus relative pressure P/P_0 are presented using specular X-ray reflectivity (SXR). Finally, the well-known Kelvin equation is applied to the SXR adsorption data to obtain a PSD for comparison to the SANS results.

Experimental Section[3]

Materials. The spin-on MSQ low-k dielectric sample on a silicon substrate was obtained from International SEMATECH. The atomic composition of the sample was determined by an established ion scattering technique.[4] The measured film atomic composition was 0.18 Si, 0.35 O, 0.10 C, and 0.37 H by mole fraction. The standard uncertainties in the atomic composition are ±0.05 by mole fraction, representing one standard deviation based on the goodness of typical fits to the data. The dielectric constant of the material quoted by the supplier was $k = 2.4$. Toluene-h_8 and toluene-d_8 (99+ atom % d) were obtained from Sigma-Aldrich, Inc.

SXR. SXR data were obtained using a custom-built high-resolution reflectometer capable of characterizing films up to 1.5-μm thick. Data were collected in the specular condition with the grazing incident angle equal to the detector angle. The film thickness, surface roughness, and electron density profile were deduced using a computer modeling routine (*mlayer*) developed at NIST to fit the experimental data. The overall pore volume fraction and solvent uptake were deduced from the calculated electron densities. The standard uncertainties in pore volume fractions are estimated to be (±0.014) and represent one standard deviation based on the goodness of typical fits to the SXR data. To estimate the solvent volume fraction ϕ_s as a function of relative pressure P/P_0, SXR porosimetry was conducted by one of two methods. In the "pressure variation" (PV) method, a stream of saturated toluene in dry air (at constant partial pressure P_0) from a bubbler held at 25 °C was combined with a second stream of pure air to control solvent partial pressure. The relative pressure of solvent was increased in increments from $P/P_0 = 0.0$ (pure air) to $P/P_0 = 1.0$ (saturated toluene) by controlling the flow rates of the air and saturated toluene streams. In the "temperature variation" (TV) method, a stream of saturated toluene vapor from a bubbler held at 30 °C was passed through the sample chamber at a flow rate of 500 cm^3 min^{-1}, and P/P_0 was varied by changing the sample temperature, effectively changing P_0 inside the pores. In both types of experiments, the vapor delivery apparatus consisted of two mass flow controllers (MKS Instruments, Inc.). The total flow rate was maintained at 500 cm^3 min^{-1}.

SANS. SANS measurements were conducted at the National Institute of Standards and Technology Center for Neutron Research 8 m Small-Angle Neutron Scattering facility.[5,6] A sample-to-detector distance of 384 cm was employed. The neutron wavelength was $\lambda = 6$ or 9 Å with a spread of $\Delta\lambda/\lambda = 0.12$. Data processing was conducted using software provided by the Center for Neutron Research at NIST. The number of counts was corrected for detector sensitivity, background scattering, and empty cell effects. Absolute scattering intensities were calculated by comparison to the empty beam intensity, and data were corrected using the experimental values for sample transmissions. The resulting data sets were circularly averaged to yield the absolute scattered intensity, $I(q)$, as a function of the scattering vector, q. Fits to the scattering data were made by a least squares regression, giving an average and a standard deviation to the fit. The relative uncertainties reported are one standard deviation, based on the goodness of the fit. Total combined uncertainties from all external sources are not reported, because comparisons are made with data obtained under the same conditions. In cases where the limits are smaller than the plotted symbols, the limits are left out for clarity.

The low-k thin film sample was obtained from International SEMATECH on a 0.725-mm-thick silicon substrate. The sample was cut into multiple circular disks of approximately 2 cm diameter. SANS measurements were conducted on a stack of 10 identical films to increase the scattered intensity. The film stack was placed inside a custom-built flow-through stainless steel scattering cell equipped with quartz windows. The cell was made leak-tight by compression of the solvent-resistant rubber O-rings against the quartz windows. The flow-through assembly was placed under a vacuum during SANS experiments to eliminate scattering from air and to permit removal of an unnecessary optical component from the beam path. The samples remained at approximately atmospheric pressure during experiments, and vapor flow through the cell was verified by use of an exit bubbler.

SANS porosimetry experiments were conducted using a "contrast match" toluene mixture. The composition of the contrast match toluene mixture was determined in an earlier study to be 0.22 toluene-d_8/0.78 toluene-h_8 by mole fraction.[7] In a fashion similar to the SXR porosimetry experiments, P/P_0 could be varied by either the PV or the TV technique. Porosimetry data were collected at P/P_0 increments of 0.1 or at P/P_0 increments of 0.05 in cases where the scattered intensity was a strong function of P/P_0.

For PV porosimetry, the solvent vapor was delivered to the samples by use of two syringe pumps with adjustable flow rates. The syringe pumps were equipped with 100-cm^3 syringes. One syringe contained 1−2 cm^3 of contrast match toluene in equilibrium with a comparatively large volume of saturated vapor. The other syringe contained air and was lubricated with vacuum grease to discourage leaking through the ground glass joint. The relative pressure P/P_0 of the contrast match solvent in the effluent could be varied by mixing the air and solvent vapor streams at different flow rates. After waiting approximately 60 min for the sample to equilibrate at a given P/P_0, SANS data were collected. In cases where the equilibration of the sample with the vapor was in doubt, the SANS data was collected for an extended period of time until no further change in the scattered intensity was noted. Since the time of this study, a second-generation automated vapor delivery apparatus similar to the SXR porosimetry equipment has been constructed using mass flow controllers equipped with solvent bubblers.

For porosimetry by the TV method, saturated toluene vapor of the contrast match composition was delivered to the sample by use of a glass bubbler maintained at 30 °C. The sample temperature was varied from 30.0 to 125.0 °C, effectively changing P_0 inside the pores. In data analysis, a value of P equal to the vapor pressure of toluene at 30 °C was assumed.

Results and Discussion

SANS Contrast Variation. Neutron scattering is a valuable technique for the quantitative measurement of pore size in thin films that we have recently applied to low-k dielectrics.[7] SANS measurements on thin film samples are conducted with the neutron beam perpendicular to the surface of the thin film, which is cast upon

(3) Certain commercial materials and equipment are identified in this paper to adequately specify the experimental procedure. In no case does such identification imply recommendation by the National Institute of Standards and Technology nor does it imply that the material or equipment is the best available for this purpose.

(4) Composto, R. J.; Walters, R. M.; Genzer, J. *Mater. Sci. Eng. R* **2002**, *38*, 107−180.

(5) Hammouda, B.; Krueger, S.; Glinka, C. J. *J. Res. Natl. Inst. Stan.* **1993**, *98*, 31−46.

(6) Prask, H. J.; Rowe, J. M.; Rush, J. J.; Schroeder, I. G. *J. Res. Natl. Inst. Stand. Technol.* **1993**, *98*, 1−13.

(7) Hedden, R. C.; Lee, H.-J.; Bauer, B. J. *Langmuir* **2004**, *20*, 416−422.

a single-crystal silicon substrate. The silicon substrate is nearly neutron-transparent, and surface scattering from the film is insignificant compared to that encountered with powdered samples because the surface/volume ratio is much smaller for a thin film. Therefore, the coherent part of the scattered intensity largely arises from the internal structure of the film(s). Contrast between the matrix (or "wall") of the porous material and the pores generates a substantial amount of coherent scattering. An average pore size is found by fitting the data to an appropriate scattering model. By filling the pores with solvents of varying SLD, a procedure known as "contrast variation", it is also possible to characterize matrix homogeneity and density. In some cases, it may be possible to identify "closed pores", defined here as pores inaccessible to solvent.

Previously, we applied contrast variation SANS to characterize four low-k dielectric thin films.[7] By filling pores with mixtures of toluene-d_8 (high SLD) and toluene-h_8 (low SLD), it was possible to vary the contrast of the filled pores with respect to that of the matrix. Pore filling was achieved by adsorption of saturated vapor by the same procedure used in the current study. The previous work concluded that all pores were accessible to the toluene in each of the materials studied; no evidence of closed porosity was detected. The tendency of toluene to fill the pores completely probably arises from its ability to wet the surface of the low-k materials. In addition, a slight solubility of toluene in the matrix of the low-k dielectrics in ref 7 is likely, perhaps allowing pores to fill even if they are not directly connected to the surface. Toluene is also a desirable choice of solvent because it does not have acidic protons/deuterons under the conditions employed in these experiments, so the risk of $h-d$ exchange between solvent and sample is minimized.

The low-k dielectric sample in the current study is the same material as the MSQ material in ref 7. A "contrast match" solvent mixture of 0.78 toluene-h_8/0.22 toluene-d_8 by mole fraction was previously identified for this sample. When pores were filled with toluene of this composition, only negligible coherent scattered intensity remained. This observation indicated that the solvent-filled sample was homogeneous in neutron SLD. Therefore, the sample matrix was essentially homogeneous in atomic composition, and all of the pores must have filled with toluene. If either unfilled pores or compositional inhomogeneities were present, then a contrast match point would not exist. The observation of a true contrast match point is a prerequisite for application of the SANS porosimetry technique presented in this paper. If compositional inhomogeneities or closed pores exist, the SANS porosimetry analysis may become intractable because of the complexity of scattering from a multiphase material.[8] Thus, it is fair to say that the SANS porosimetry technique is essentially limited to materials with a homogeneous matrix and solvent-accessible pores. In addition, the pore size must lie in the range appropriate for SANS experiments, or about 10 to several thousand Å.

The MSQ dielectric used in this study has a random two-phase morphology that could be well represented by a fit to the Debye−Anderson−Brumberger (DAB) expression:[9]

$$I(q) = \frac{8\pi\phi_0(1-\phi_0)(\rho_m\sigma_m - \rho_s\sigma_s)^2\xi^3}{(1+\xi^2q^2)^2} \qquad (1)$$

In eq 1, ϕ_0 is the volume fraction of pores, ξ is the correlation length, ρ_m and ρ_s are the mass densities of the film matrix (wall) and the solvent, and σ_m and σ_s are the total neutron scattering lengths per unit mass of the matrix and the solvent. The best fit to the scattering data for the MSQ dielectric under a vacuum (empty pores) gave a correlation length of $\xi = 44.4 \pm 0.2$ Å. The correlation length is a composite phase size for the material including both pore and matrix phases. For a randomly structured two-phase porous material, the average pore size is most easily expressed as an average chord length, l_c, given by

$$l_c = \xi/(1-\phi_0) \qquad (2)$$

where ϕ_0 is the overall volume fraction of pores. The overall porosity of this MSQ sample as determined by X-ray reflectivity[7] is $\phi_0 = 0.309 \pm 0.014$.

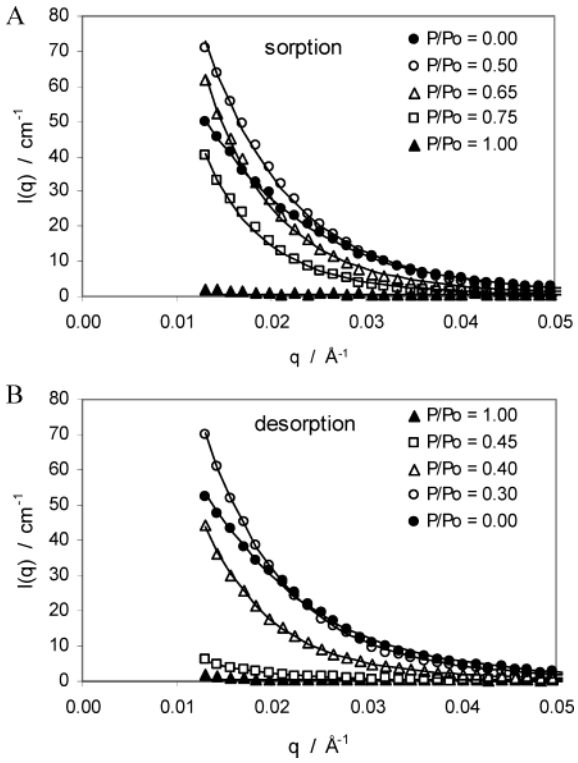

Figure 1. Dependence of scattered intensity $I(q)$ on solvent relative pressure P/P_0 for SANS porosimetry experiments of the PV method. A: Adsorption data (increasing P/P_0). B: Desorption data (decreasing P/P_0). Lines are fits to the DAB expression (eq 2). When all pores are filled with contrast match solvent ($P/P_0 = 1$), the scattered intensity approaches 0 over all q.

SANS Capillary Porosimetry. After contrast variation experiments identified a true contrast match point, the PSD of the MSQ dielectric was probed by SANS capillary porosimetry. Porosimetry was conducted using the contrast match toluene mixture as a "probe" solvent. There are two techniques by which the toluene P/P_0 was varied: the PV method and the TV method, which are described in detail in Experimental Section. The two methods should represent thermodynamically equivalent ways to vary P/P_0. Data from both experimental methods are illustrated here for the sake of completeness.

Figure 1A shows SANS data for the adsorption process using the PV technique. The partial pressure P of the solvent vapor in air was varied incrementally by mixing saturated solvent vapor (in air) with a stream of pure air.

(8) Wu, W. L. *Polymer* **1982**, *23*, 1907−1912.
(9) Debye, P.; Anderson, H. R.; Brumberger, H. *J. Appl. Phys.* **1957**, *28*, 679.

The sample temperature and the saturated solvent vapor pressure P_0 were held fixed. For clarity, only selected data sets are plotted to illustrate how the scattered intensity varied with P/P_0. As P/P_0 increased from 0.0 to 0.5, $I(q)$ increased over all q in the q range measured, more so at low q, as the smallest pores filled with contrast match liquid. This increase in the scattering with increasing P/P_0 may be attributed to the filling of micropores (tiny pores of radius $\leq$10 Å), which would increase the correlation length ξ. It is quite possible that the present sample contains some microporosity, as many MSQ materials do contain tiny cagelike structures. One might assume that filling the smallest pores would cause a decrease in the scattered intensity, in particular at the high end of the q range (which is outside of the measured range). However, according to eq 1, $I(q)$ depends on ξ^3, so any increase in the correlation length causes a dramatic increase in the scattered intensity. In contrast, the decrease in the unfilled pore volume fraction upon filling of the micropores causes a relatively weak change in $I(q)$. In addition, the magnitude of $I(q)$ depends on the contrast between the empty mesopores and the surrounding matrix (including micropores). Filling of the micropores with solvent is essentially equivalent to adding SLD to the matrix without filling any of the mesopores. The contrast of the empty mesopores with the surrounding matrix increases, and $I(q)$ correspondingly increases over the measured q range. Any decrease in scattered intensity due to filling of the micropores at very high q cannot be measured under the experimental conditions employed.

As P/P_0 increased to 0.65 and then 0.75, the scattered intensity decreased over all q. This decrease in intensity was due primarily to a substantial decrease in the volume fraction of empty pores. At $P/P_0 = 1$, all of the pores were filled with solvent, and the scattered intensity was close to 0 over all q. Porosimetry experiments were then repeated in reverse order (desorption branch, Figure 1B), starting from $P/P_0 = 1$ and working toward $P/P_0 = 0$. During desorption, little change in the scattering was observed as P/P_0 decreased incrementally from 1.0 to 0.5, indicating that essentially all of the pores remained filled with the contrast match solvent. The first significant change in the scattering, indicating the onset of the unfilling or emptying process, was noted at $P/P_0 = 0.45$. As P/P_0 decreased to 0.4 and 0.3, dramatic increases in the scattered intensity were observed as the largest pores emptied. As P/P_0 approached 0 and all of the pores emptied, the scattering curve resumed its original shape, supporting the idea that the solvent adsorption did not deform or otherwise alter the sample.

The SANS porosimetry measurements were repeated using the TV method to vary P/P_0. A stream of saturated toluene vapor in air maintained at a constant temperature (30 °C) was passed over the sample while the sample temperature was changed incrementally. This procedure changes the saturated vapor pressure of the solvent P_0 inside the pores while the external partial pressure P is held fixed. As the sample temperature is increased, P/P_0 decreases, and as temperature decreases, P/P_0 increases. The saturated vapor temperature was maintained at 30 °C while the sample temperature was increased incrementally from 30 to 125 °C. In data analysis, a value of P equal to the vapor pressure of toluene at 30 °C was assumed. This assumption is best in the limit of very high vapor flow rate through the cell. However, some heating of the external vapor near the sample surface is unavoidable, especially at $T \gg 30$ °C, reducing the value of P. One can calculate a corrected P/P_0 for the extreme case where the external vapor is heated to the sample temperature.

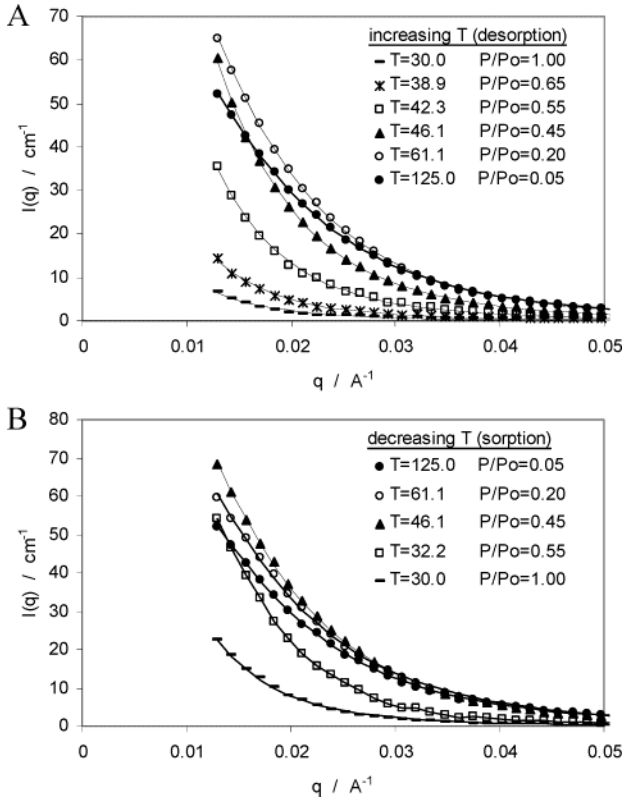

Figure 2. Dependence of scattered intensity $I(q)$ on solvent relative pressure P/P_0 for SANS porosimetry experiments of the TV method. A: Adsorption data (decreasing T, increasing P/P_0). B: Desorption data (increasing T, decreasing P/P_0). Lines are fits to the DAB expression (eq 2).

Even in this worst case, the correction to P/P_0 is not enough to drastically alter the adsorption data, so the authors proceeded without applying any correction for vapor heating. Using published data to estimate $P_0(T)$,[11] the ratio of P/P_0 was decreased from 1.00 to 0.033 (desorption branch). By decreasing the temperature from 125 back to 30 °C, adsorption data were obtained over the same range of P/P_0. Figure 2A shows SANS data for increasing temperature (desorption), and Figure 2B shows the data for decreasing temperature (adsorption). A discrepancy should be mentioned: at 30 °C ($P/P_0 = 1.0$) in the TV experiments, the contrast match point was not reached as it was in the PV experiments at (23.0 °C). A very significant error in determining the match point composition would be needed to cause such a departure from the contrast match condition, which is unlikely. On the other hand, a small number of large unfilled pores could account for the difference. The existence of a population of unfilled pores of relatively large size may be attributed to a slight discrepancy between the sample temperature and bubbler temperature. The effective value of P/P_0 is very sensitive to slight differences in temperature when the sample and bubbler are at approximately the same temperature. The authors chose to proceed with data analysis despite the lack of a true contrast match point at $P/P_0 = 1.0$.

Quantitative comparison between the data obtained by the PV and TV methods was accomplished by fitting the data to the DAB model (eq 2). For each value of P/P_0, $I(q=0)$ and a correlation length ξ were fitted to eq 2 by a

(10) Gregg, S. J.; Sing, K. S. W. *Adsorption, Surface Area and Porosity*, 2nd ed.; Academic Press: London, 1982.

(11) Vargaftik, N. B. *Tables on the Thermophysical Properties of Liquids and Gases (English Translation)*, 2nd ed.; Hemisphere Publishing Corp.: Washington, DC, 1975; p 348.

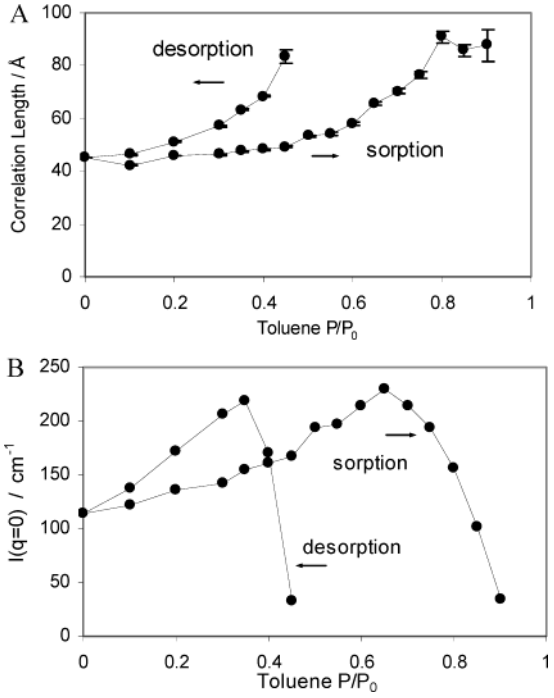

Figure 3. Fitted correlation length ξ and zero-angle scattered intensity $I(q=0)$ from the DAB expression (eq 2) for contrast match SANS porosimetry data obtained using the PV method to vary P/P_0. See Experimental Section for explanation of uncertainties. Lines are a guide to the eye.

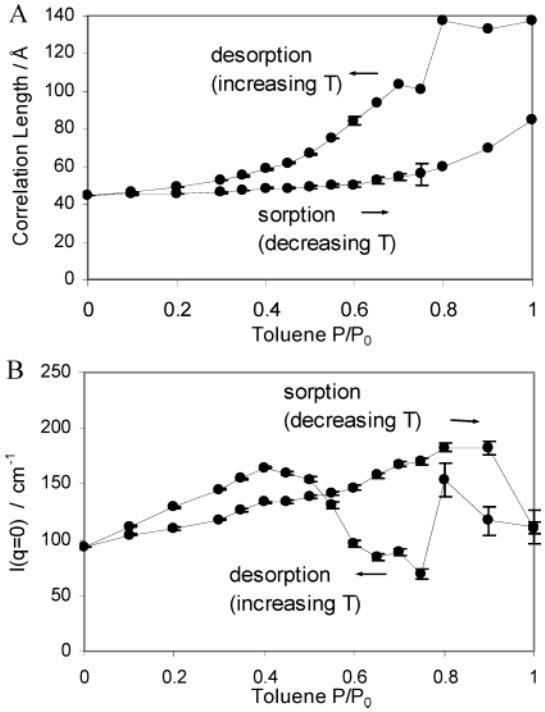

Figure 4. Fitted correlation length ξ and zero-angle scattered intensity $I(q=0)$ from the DAB expression (eq 2) for contrast match SANS porosimetry data obtained using the TV method to vary P/P_0. See Experimental Section for explanation of uncertainties. Lines are a guide to the eye.

nonlinear least squares regression. The lines in Figures 1 and 2 are the best fits to eq 2 over the range $0.012 < q < 0.14$ Å^{-1}. Interestingly, the scattering was well-represented by the DAB model over the q range studied at all values of P/P_0. Judging by the goodness of the fits, a random two-phase structure was apparently maintained regardless of the amount of filled pores.

Figure 3 shows the fitted values of correlation length and $I(q=0)$ for the PV method as a function of P/P_0. A clear hysteresis is observed in both plots. The adsorption process is accompanied by a gradual increase in the correlation length as pores fill with contrast match solvent from smallest to largest, followed by only slight changes in the fitted correlation length above $P/P_0 = 0.8$, where the vast majority of the pores are filled. Judging by the weakness of the scattered intensity at $P/P_0 = 1$ (Figure 1), all of the pores were filled with contrast match solvent. In contrast, the desorption process is characterized by an abrupt change in correlation length near $P/P_0 = 0.45$ accompanying an emptying of a substantial volume fraction of the pores. At $P/P_0 > 0.45$, all pores are filled with contrast match solvent. In such cases, the scattered intensity was very weak (similar to the bottom curve in Figure 1B at $P/P_0 = 1.0$), and our fits to the DAB expression did not converge properly. It was not possible to determine reliable values for $I(q=0)$ and ξ in situations where all of the pores were filled with solvent. However, it is doubtful that the fitted parameters would have any physical meaning anyway. Because $I(q=0)$ and ξ could not be determined reliably at $P/P_0 = 1.0$, no values are plotted in Figure 3. Similarly, in the desorption data, the fits to the DAB expression did not converge reliably above $P/P_0 = 0.45$, so no data are shown in Figure 3. For data in Figure 3, error bars represent one standard deviation based on the goodness of the fits and do not reflect the total combined uncertainty for all sources.

The SANS data obtained by the TV method were fitted to the DAB expression in a similar fashion. Figure 4 shows the fitted values of correlation length and $I(q=0)$ for the TV method as a function of P/P_0. The data are qualitatively similar to those from the PV method only in that hysteresis is observed. Comparing the PV and TV porosimetry experiments, the pore filling process must follow different pathways as P/P_0 is varied. At the present time, the authors cannot explain the physical basis for the differences in the data sets. In the TV experiments, there was no problem with convergence of the fits to the DAB expression as we encountered in some of the data sets in the PV experiments. Because a perfect contrast match point was not observed, as discussed earlier, $I(q=0)$ never approached 0, the limit where convergence was problematic. Thus, fitted values for $I(q=0)$ and ξ can be shown over the entire range of P/P_0. Note that $I(q=0)$ does not approach 0 as P/P_0 approaches 1.0, suggesting again that some of the pores may have remained unfilled.

Adsorption Data from SXR. Further information about the pore filling process was obtained by use of SXR to measure the uptake of solvent in the film as a function of P/P_0. Recently, SXR has emerged as a quantitative analytical technique for analysis of pore and matrix characteristics in low-k dielectrics. SXR porosimetry has been applied to measure film thickness, pore volume fraction, matrix mass density, coefficient of thermal expansion, and solvent/moisture uptake in low-k dielectrics.[12−18]

(12) Lee, H.-J.; Lin, E. K.; Bauer, B. J.; Wu, W.-L.; Hwang, B. K.; Gray, W. D. *Appl. Phys. Lett.* **2003**, *82* (7), 1084−1086.

(13) Lee, H.-J.; Kim, Y.-H.; Kim, J. Y.; Lin, E. K.; Bauer, B. J.; Wu, W.-L.; Kim, H. J. *Proceedings of the IEEE International Interconnect Technology Conference, 5th*, Burlingame, CA, June 3−5, 2002, pp 54−56.

(14) Lee, H.-J.; Soles, C. L.; Liu, D. W.; Bauer, B. J.; Wu, W.-L. *J. Polym. Sci., Part B: Polym. Phys.* **2002**, *40* (19), 2170−2177.

(15) Lin, E. K.; Lee, H.-J.; Lynn, G. W.; Wu, W.-L.; O'Neill, M. L. *Appl. Phys. Lett.* **2002**, *81* (4), 607−609.

In the current study, SXR is useful to quantify the volume fraction of solvent ϕ_s in the film as a function of P/P_0. This "X-ray porosimetry" technique and its application to low-k dielectrics have been described in more detail elsewhere.[13,14] The SXR measurement yields an average electron density for the film, including any adsorbed solvent molecules. Fits to the SXR data provide a critical angle θ_c, below which total external reflection occurs. The angle θ_c is related to the bulk electron density in the films

$$\rho_{el} = \frac{\pi\theta_c^{\,2}}{\lambda^2 r_e} \tag{3}$$

In eq 3, λ is the X-ray wavelength (1.54 Å), θ_c is the critical angle in rad, and r_e is the radius of an electron, taken as 2.82×10^{-5} Å. To determine solvent uptake at a give value of P/P_0, the electron density of the film is first measured in the absence of solvent (under a vacuum) and then at P/P_0. Knowing the number of electrons per solvent molecule, the number density of solvent molecules in the film at P/P_0 can be calculated. The increase in the film electron density upon filling the pores is proportional to the total number of solvent molecules in the film. The number of solvent molecules per unit volume in the film is given by

$$\frac{\text{solvent molecules}}{\text{volume}} = \frac{\rho_{el}^{\,P/P_0} - \rho_{el}^{\,vac}}{n_{el}} \tag{4}$$

In eq 4, $\rho_{el}^{\,P/P_0}$ is the electron density of the film when exposed to solvent at relative pressure P/P_0, ρ_{el}^{vac} is the electron density of the film in a vacuum, and n_{el} is the number of electrons per solvent molecule. If the mass density of the solvent inside the pores is assumed to be the same as its bulk mass density ρ_s, then the volume fraction of the solvent in the film at P/P_0 is given by

$$\phi_s = \left(\frac{\rho_{el}^{\,P/P_0} - \rho_{el}^{\,vac}}{n_{el}}\right)\left(\frac{M_s}{N_A\rho_s}\right) \tag{5}$$

where M_s is the molar mass of the solvent and N_A is Avogadro's number.

At any given value of P/P_0, the volume fraction of solvent in the film ϕ_s is determined using eqs 3−5. The overall pore volume fraction in the film ϕ_0 is calculated from eq 5 by measuring the film electron density at $P/P_0 = 1$ (saturated vapor, liquid-filled pores). All of the pores are assumed to be filled with solvent at $P/P_0 = 1$, so the volume fraction of solvent ϕ_s given by eq 5 is equal to the total pore volume fraction ϕ_0. On the basis of the observation of a true contrast match point for the MSQ film in this study, it is reasonable to assume that all of the pores are filled with liquid when exposed to saturated toluene vapor. An overall pore volume fraction of $\phi_0 = 0.309 \pm 0.014$ was calculated for the MSQ film using saturated toluene vapor at 25 °C. At any value of P/P_0, ϕ_s is the volume fraction of solvent-filled pores, the quantity $\phi_0 - \phi_s$ is the volume fraction of empty pores, and the quantity $1 - \phi_0$ is the volume fraction of the matrix.

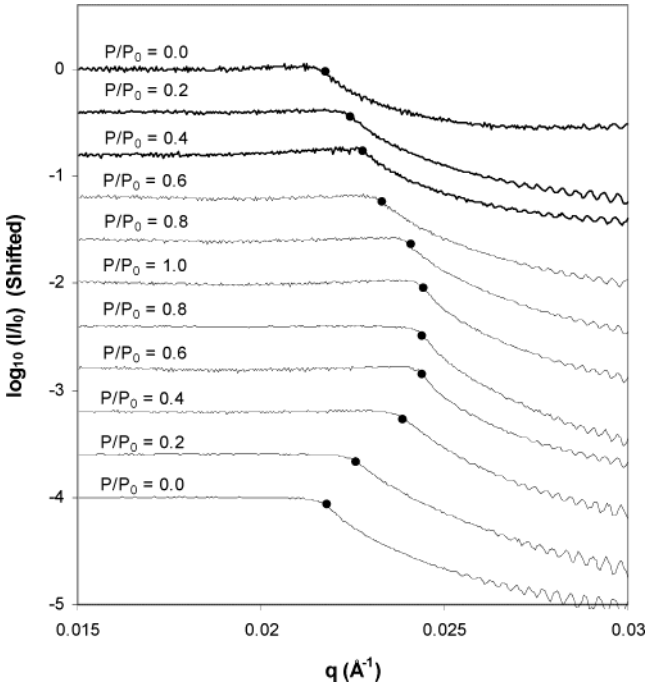

Figure 5. SXR porosimetry data for the MSQ dielectric. Connecting lines are shown instead of individual data points for clarity. Black dots represent best-fit values for q_c.

Figure 5 shows SXR data [log(reflected intensity/incident intensity) vs momentum transfer q] for the toluene porosimetry experiment using the PV technique to vary P/P_0. The critical q (the value of q at which the initial sharp drop in reflectivity occurs) or q_c is the point below which total external reflection of the X-rays occurs and above which the X-rays penetrate the film. q_c is related to the critical angle θ_c in eq 3 by $q_c = (4\pi \sin \theta_c)/\lambda$, where λ is the X-ray wavelength. The reflectivity of the film is measured as the relative pressure of the adsorbent (toluene) is increased stepwise from $P/P_0 = 0.0$ (top) to 1.0 (center) and subsequently decreased stepwise to 0.0 (bottom). The value of q_c is strongly affected by the overall film density; q_c increases as the amount of toluene in the film increases and then decreases when the toluene desorbs. Using the computer modeling routine *mlayer*, a best fit value for q_c is obtained for each P/P_0 and the volume fraction of solvent in the film is calculated by eqs 3−5. Best fit values for q_c are represented by black dots in Figure 5. Besides porosity information, the *mlayer* fits to the SXR data also yield a very precise value for the film thickness, allowing the overall film swelling to be measured. The MSQ sample in the current study varied in thickness from 10 360 ± 20 Å in the dry state to 10 440 ± 20 Å in the saturated toluene atmosphere. The minimal swelling exhibited by this material suggests that the toluene did not distort the sample substantially. In ref 7, we observed that the shape of the SANS data was unaffected upon filling the pores with toluene, and only the intensity changed. These observations support the idea that the pore structure in the MSQ material was not deformed by condensation of toluene in the pores.

Figures 6 and 7 show SXR porosimetry data for the MSQ sample using toluene-h_8 as an adsorbent by the PV and TV methods, respectively. The volume fraction of toluene in the film ϕ_s from eq 5 is plotted versus P/P_0. As with SANS experiments, SXR porosimetry data were collected using both the PV method with the sample temperature held at 25 ± 0.2 °C and the TV method with the solvent bubbler held at 30 ± 0.2 °C. As with the SANS

(16) Lee, H.-J.; Lin, E. K.; Wang, H.; Wu, W.-L.; Chen, W.; Moyer, E. S. *Chem. Mater.* **2002**, *14* (4), 1845−1852.
(17) Bauer, B. J.; Lin, E. K.; Lee, H.-J.; Wang, H.; Wu, W.-L. *J. Electron. Mater.* **2001**, *30* (4), 304−308.
(18) Lin, E. K.; Lee, H.-J.; Wang, H.; Wu, W.-L. American Institute of Physics Conference: Characterization and Metrology for ULSI Technology 2000, Gaithersburg, MD, June 26−29, 2000. *AIP Conference Proceedings* **2001**, *550*, 453−457.

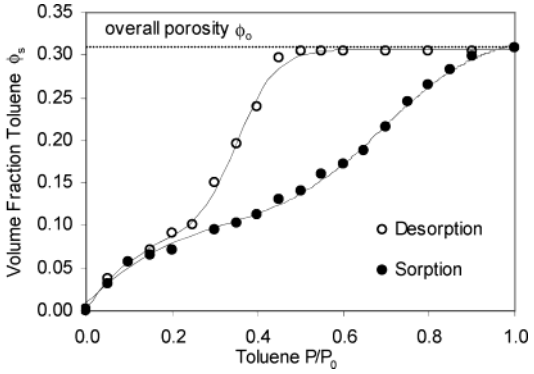

Figure 6. Adsorption data for toluene-h_8 in the nanoporous MSQ thin film obtained by SXR using the PV method to vary P/P_0. Uncertainties in ϕ_s are quoted in Experimental Section. Lines are fits to the empirical expression eq 8.

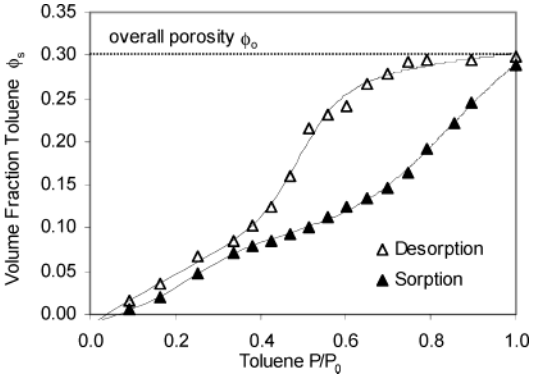

Figure 7. Adsorption data for toluene-h_8 in the nanoporous MSQ thin film obtained by SXR using the TV method to vary P/P_0. Uncertainties in ϕ_s are quoted in Experimental Section. Lines are fits to the empirical expression eq 8.

experiments, the PV and TV methods were found not to be equivalent. Compared to the PV porosimetry data at 25 °C, the TV porosimetry data gave a slightly lower overall porosity of $\phi_0 = 0.300 \pm 0.014$, but these values are equivalent within the limits of experimental uncertainty. Both data sets exhibit a prominent hysteresis loop and are representative of "Type IV" isotherms exhibited by most mesoporous solids. The data for the PV method strongly resemble the Type IV$_E$ isotherm,[10] while the TV method data have a slightly different shape. The underlying physical reason for the difference in shape is not clear at the present time.

The hysteresis phenomenon in mesoporous solids arises because pore filling by capillary condensation (adsorption) and evaporation of the condensed liquid (desorption) occur via different pathways. The underlying physical basis for the hysteresis has been debated, however. One explanation[10] is that during adsorption, the capillary condensation process must nucleate by adsorption of a thin layer on the pore walls before pore filling by capillary condensation can commence. In contrast, during desorption, evaporation from the filled pores occurs readily if the pressure is low enough, and there is no such nucleation process. Because condensation and evaporation from a given pore occur at different relative pressures, a hysteresis loop is observed. Alternatively, the hysteresis may be attributed to a pore-blocking mechanism or "ink-bottle" effect in certain mesoporous materials.[10,19,20] During adsorption, pores fill in order from smallest to largest as P/P_0 increases. During desorption, some amount of comparatively large pores below the surface are shielded from the external atmosphere because the pathway to the surface is blocked by smaller pores or bottlenecks filled with liquid. Thus, the evaporation of liquid from the larger pores may occur at lower values of P/P_0 that what would be observed if all pores were readily accessible from the surface. Without specific knowledge of the pore geometry in a given material, it is difficult to assign a mechanism to the hysteresis loop. For the MSQ material in the current study, all that is known about the pore structure is that the pores form a random structure (are not ordered). Both the "nucleation" and "ink bottle" effects may or may not contribute to the observed hysteresis. Further interpretation of the cause of the hysteresis loop observed would require more specific knowledge of the pore geometry.

Combination of SANS and SXR Porosimetry Data. Size information from SANS can be combined with the solvent uptake data from SXR to characterize the pore filling process. The SXR data was used to convert the correlation length ξ from SANS to a more intuitive parameter describing pore size: the average chord length, l_c. For a random two-phase material with irregularly shaped pores, the average length of chords passing through the pores is perhaps the most meaningful parameter to describe pore size. When pores are irregularly shaped, interconnected, and/or of unknown morphology, it is difficult to define any other measure of pore size. For a random porous material with a homogeneous matrix, the average chord length is given by eq 2 when all pores are empty. For a SANS porosimetry experiment with a contrast match solvent, the solvent-filled pores match the matrix and, therefore, are not included in the volume fraction of the pore phase, so the average chord length is actually given by

$$l_c = \frac{\xi}{1 - (\phi_0 - \phi_s)} \tag{6}$$

where the quantity $\phi_0 - \phi_s$ is the empty pore volume fraction. The solvent uptake information from SXR provides accurate values for both the volume fraction of solvent in the film, ϕ_s, and the overall pore volume fraction, ϕ_0.

Using the SXR measurement of $\phi_0 - \phi_s$, all correlation lengths from SANS were converted to average chord lengths by eq 6. A plot of average chord length versus empty pore volume fraction characterizes the pore filling process (Figure 8). The abscissa in Figure 8 is $(\phi_0 - \phi_s)/\phi_0$, or the fraction of the pores that are empty (by volume). The condition $(\phi_0 - \phi_s)/\phi_0 = 1$ corresponds to the condition where all pores are empty, as at $P/P_0 = 0$. The condition $(\phi_0 - \phi_s)/\phi_0 = 1$ corresponds to the condition where all pores are liquid-filled, as at $P/P_0 = 1$. Interestingly, the data from the TV and PV methods appear to collapse to a single curve when plotted in this fashion. This may result because the SANS measurement characterizes the average size of the empty portion of the pores irrespective of the pathway followed by the adsorption process. In addition, the adsorption and desorption data also appear to lie on the same curve within the limits of uncertainty. By eliminating the P/P_0 variable and plotting the data in this fashion, the ambiguities introduced by the hysteresis phenomenon were circumvented, at least for the MSQ material in this study.

Looking at the right side of Figure 8, the overall average chord length when most or all of the pores are empty is approximately 55−65 Å. Moving from the right side of

(19) de Boar, J. H. In *The Structure and Properties of Porous Materials*; Everett, D. H., Stone, F. S., Eds.; Butterworth: London, 1958; p 68.
(20) Everett, D. H. In *The Solid-Gas Interface*; Flood, E. A., Ed.; Dekker: New York, 1967; Vol. 2, p 1055.

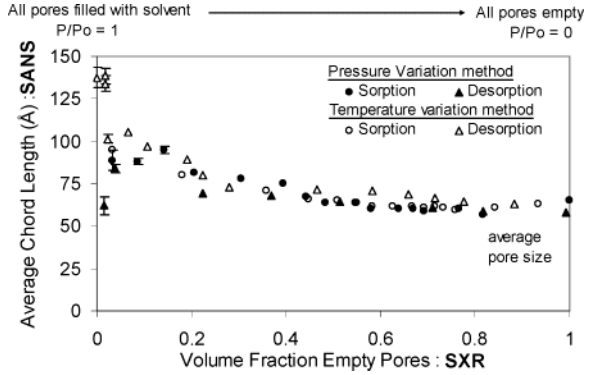

Figure 8. Size dependence of the pore filling process during a porosimetry experiment. Average pore size (chord length) was determined by eq 8 using the SANS correlation length, and the volume fraction of empty pores was measured by SXR. The right side of the chart corresponds to the condition $P/P_0 = 0$ where all of the pores are empty, while the left side corresponds to $P/P_0 = 1$ where all of the pores are filled with liquid. Error bars are based on the goodness of the fits to the data and do not reflect the total combined uncertainty.

Figure 8 to the left describes the variation of average pore size as pores are filled with contrast match solvent. Judging by the data near $(\phi_0 - \phi_s)/\phi_0 = 0.5$, where half the volume of pores has been filled with contrast match solvent, the measured average size of the remaining empty pores is only slightly higher. Because the smallest pores are expected to preferentially fill with solvent first, this observation suggests that the overall shape of the SANS data is not strongly affected by the smallest pores. The filling of the smallest pores in this material results in a substantial increase in $I(q=0)$ but relatively little change in the correlation length from the fits to the DAB expression, which is insensitive to subtle changes in the shape of the scattering data at high q. These observations suggest that there may be a population of very small pores with diameter less than about 10 Å, which is the approximate lower size limit of the SANS technique.

As the empty pore fraction $(\phi_0 - \phi_s)/\phi_0$ approaches 0, the upper end of the PSD is probed. The limit of l_c as $(\phi_0 - \phi_s)/\phi_0 \rightarrow 0$ theoretically gives the size of the largest pores in the distribution, although statistics may not be good enough to permit a meaningful extrapolation. As the empty pore volume fraction approaches 0, the total combined uncertainty in the average chord length invariably increases, as evidenced by the increased scatter in the data at the left side of Figure 8. This deterioration in the quality of the data is due to the decrease in scattered intensity when only a small population of empty pores remains. Extrapolating the data in Figure 8 visually suggests that there are at least some pores present in the MSQ material with a chord length in excess of 100 Å.

Capillary Porosimetry and the Kelvin Equation. A simple physical model frequently chosen to analyze adsorption data is the classical Kelvin equation. The Kelvin equation is derived by considering the shape of a vapor−liquid interface inside a pore and applying the Young−Laplace equation to calculate the (reduced) equilibrium vapor pressure above the interface.

$$\ln\left(\frac{P}{P_0}\right) = -\left(\frac{\gamma V_m}{RT}\right)\left(\frac{1}{r_1} + \frac{1}{r_2}\right) \qquad (7)$$

In eq 7, γ is the surface tension of the solvent, V_m is the solvent molar volume, and r_1 and r_2 are the principal radii of curvature of the liquid meniscus. For pores of simple geometry, eq 7 is often written as

$$\ln\left(\frac{P}{P_0}\right) = -\left(\frac{\gamma V_m}{RT}\right)\left(\frac{f}{r_k}\right) \qquad (7b)$$

where r_k is the "Kelvin radius". The constant f has a value of 2 for cylindrical pores or 1 for flat channel pores. In a porosimetry experiment, the Kelvin radius governing capillary condensation may be less than the pore radius because of a layer of adsorbed solvent on the pore wall. The radius of the pore is related to the Kelvin radius by $r = r_k + t$, where t is the thickness of the adsorbent layer on the pore wall. To correct for this effect, the thickness t may be calculated from an adsorption model, but we will take t to be negligible in the current analysis for the sake of simplicity, so $r = r_k$.

According to the Kelvin eq, at any given value of P/P_0, pores of radius smaller than r_k are assumed to fill with solvent because the vapor pressure of the solvent is effectively reduced by confinement inside the mesopores. As P/P_0 increases, pores fill with liquid in order from smallest to largest. The measured mass uptake of solvent in a porous material at a given value of P/P_0 is then proportional to the volume fraction of pores of radius less than or equal to r_k. By measuring solvent uptake as P/P_0 is incremented, a size distribution can be constructed by plotting the differential uptake of solvent versus r_k. While this procedure provides a means to rapidly convert adsorption data to a size distribution, reliance on the Kelvin equation imposes major limitations on the accuracy of the measurement. From the point of view of data interpretation, the adsorption hysteresis exhibited by most mesoporous materials introduces serious ambiguities.[10] Because the adsorption and desorption branches do not follow the same path, two different PSD are calculable from the two branches. In addition, the applicability of the Kelvin equation on the <20 Å length scale is questionable because the concept of a liquid meniscus is ill-defined when working at a molecular-level scale. Because of these limitations, the PSDs reported from capillary porosimetry experiments are often not quantitative, especially in the limit of very small pore size. However, despite these limitations, the Kelvin equation has been applied to adsorption data to estimate pore size in mesoporous low-k dielectrics.[21−24] This procedure is valuable as a rapid means of comparing samples in an industrial setting, but it has some serious shortcomings if a quantitative PSD is needed.

For comparison to the SANS size measurements, a PSD was also calculated directly from the SXR porosimetry data in Figures 6 and 7 using the Kelvin equation. The version of eq 7b used assumes that pores are cylinders of infinite length ($f = 2$), which is probably not a good model for the MSQ dielectric in the present study, nor for any of the low-k dielectrics developed in recent years. The infinite cylinder geometry is used as an example here only because this model was employed in recent studies of low-k dielectric thin films by ellipsometric porosimetry.[23] This exercise is only intended to illustrate the ambiguities associated with the classical Kelvin equation analysis.

(21) Grill, A.; Patel, V.; Rodbell, K. P.; Huang, E.; Baklanov, M. R.; Mogilnikov, K. P.; Toney, M.; Kim, H.-C. *J. Appl. Phys.* **2003**, *94* (5), 3427−3435.
(22) Baklanov, M. R.; Mogilnikov, K. P. *Microelectron. Eng.* **2002**, *64* (1−4), 335−349.
(23) Baklanov, M. R.; Mogilnikov, K. P.; Polovinkin, V. G.; Dultsev, F. N. *J. Vac. Sci. Technol., B* **2000**, *18* (3), 1385−1391.
(24) Dultsev, F. N.; Baklanov, M. R. *Electrochem. Solid-State Lett.* **1999**, *2* (4), 192−194.

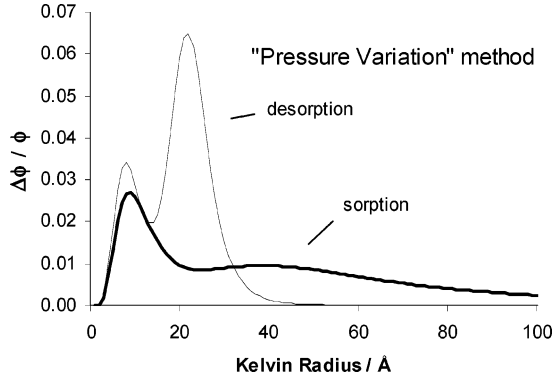

Figure 9. PSDs obtained by applying the Kelvin equation to SXR adsorption data obtained by the PV method to vary P/P_0. Solvent uptake versus P/P_0 data were fitted to the empirical expression eq 8 and then converted to a size distribution by application of eq 1.

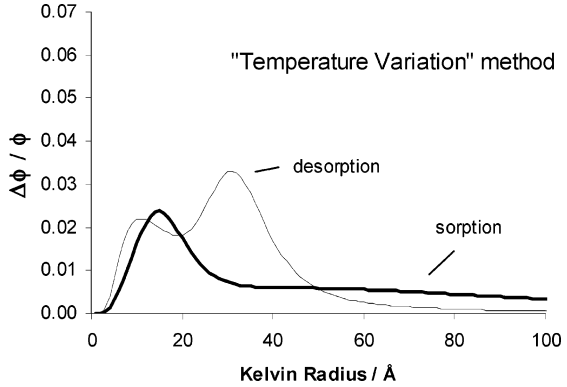

Figure 10. PSDs obtained by applying the Kelvin equation to SXR adsorption data obtained by the TV method to vary P/P_0. Solvent uptake versus P/P_0 data were fit to the empirical expression eq 8 and then converted to a size distribution by application of eq 1.

To obtain the size distribution, quantity the P/P_0 is eliminated in favor of the Kelvin radius r_k using eq 7b, and the differential solvent uptake $\Delta\phi_s$ due to filling of pores of radius between r_k and $r_k + \Delta r_k$ is plotted versus r_k. The differential uptake $\Delta\phi_s$ could be calculated directly from the porosimetry data by point-by-point differentiation, but this procedure magnifies the effects of scatter. Instead, the porosimetry data can be parametrized by fitting to an empirical function, which aids in interpolation of the data, producing a continuous size distribution and reducing the effects of experimental scatter. SXR porosimetry data in Figures 6 and 7 were parametrized by fitting to the empirical expression given in eq 8 using a nonlinear least squares algorithm.

$$\phi_s = A + \frac{B}{1 + \exp\{[C - (P/P_0)]/D\}} + \frac{B'}{1 + \exp\{[C' - (P/P_0)]/D'\}} \quad (8)$$

In eq 8, A, B, C, D, B', C', and D' are empirical constants used as fitting parameters. This expression was satisfactory for fitting both adsorption and desorption branches of the SXR data in Figures 6 and 7, provided that reasonable initial guesses for the fitting parameters were chosen. Lines in Figures 6 and 7 are fits to eq 8.

Using the fits, the PSD was calculated using a spreadsheet routine. For any given value of r_k, a corresponding value of P/P_0 was calculated by the Kelvin equation. The expected solvent uptake ϕ_s at each value of P/P_0 is then estimated using the fit of eq 8 to the data. The (normalized) differential solvent uptake $\Delta\phi_s/\phi_0$ was plotted versus r_k to obtain the PSD. For PV experiments, the surface tension of the solvent γ was taken to be 2.729×10^{-2} N m^{-1} for toluene-h_8 at 25 °C, and the solvent molar volume V_m was taken to be 1.069×10^{-4} m^3 mol^{-1} for liquid toluene-h_8, on the basis of its mass density of 862.3 kg m^{-3} at 25 °C. For TV experiments, data from ref 11 were used to estimate γ and V_m of toluene as a function of temperature.

Figure 9 shows the PSD calculated by application of the Kelvin equation to the porosimetry data obtained by the PV method (from Figure 6). Figure 10 shows the PSD calculated by application of the Kelvin equation to the porosimetry data obtained by the TV method (from Figure 7). Qualitatively, the PV and TV methods give similar size distributions, but the peaks of the distribution are slightly different. In both cases, the adsorption and desorption branches produce widely different results, which is expected for any material with a Type IV isotherm exhibiting a hysteresis loop.[10] The desorption data suggest that there is a population of mesopores with a relatively narrow size distribution having a relatively sharp cutoff well below $2r_k = 100$ Å, which is inconsistent with the SANS analysis. In contrast, the adsorption data suggest a broad size distribution peaked at approximately $r_k = 40$ Å and extending beyond 100 Å. Comparing the Kelvin equation PSDs to the SANS measurements in Figure 8, none of the Kelvin PSDs are entirely consistent with the SANS results, although perhaps the adsorption data are qualitatively in better agreement.

Both size distributions from adsorption and desorption data are bimodal, with a second peak at $r_k \approx 10$ Å. The Kelvin equation analysis, therefore, suggests that there may be a separate population of micropores (defined as pores of $r_k \leq 10$ Å).[2] This peak results from the initial steep increase in solvent uptake observed at low P/P_0 (Figures 6 and 7). A bimodal distribution of this nature is not necessarily inconsistent with the SANS data, even though the SANS data are well-represented by the DAB expression, which assumes a single-exponential distribution of pore sizes.[9] It is possible that micropores are present and their filling causes only subtle changes in the high-q portion of the scattering that were not detected because micropores are at the lower end of the size scale accessible to SANS. Because the fits to the DAB expression are dominated by the high intensity, low-q scattering, the fitted correlation length may, therefore, not be very sensitive to micropore filling. An alternative explanation for the second peak in the Kelvin equation size distributions could be the formation of a surface layer of adsorbed probe solvent at low P/P_0, rather than filling of micropores. No correction was applied to the Kelvin equation account for the formation of a surface layer, so it is possible that the micropore peak in the size distribution is artificial. Previous workers studying mesoporous MCM-41 materials demonstrated that inappropriate correction of the adsorption data for formation of surface adsorption layers can result in an artificial microporosity.[25]

The preceding analysis illustrates a fundamental ambiguity encountered by application of the Kelvin equation to porosimetry data with a hysteresis loop: there is no clear physical rationale for choosing between the different PSDs obtained from the adsorption and desorption branches. Recent workers studying low-k dielectrics by ellipsometric porosimetry[21−24] preferred to use desorption data, especially when a branched or interconnected

(25) Choma, J.; Jaroniec, M.; Burakiewicz-Mortka, W.; Kloske, M. *Appl. Surf. Sci.* **2002**, *196* (1−4), 216−223.

pore structure was suspected. This choice is motivated by the argument that desorption is characterized by formation of well-defined vapor−liquid interfaces at constricted points (bottlenecks) in the pore architecture, whereas the vapor−liquid interfaces formed during adsorption may simultaneously take a wide variety of different shapes.[23] Elsewhere, it has been argued that the adsorption data are more appropriate for determination of the PSD for materials with interconnected pore structure.[25,26] Because of the suspected "pore blocking" mechanism,[10] a portion of comparatively large pores below the surface are shielded from the external atmosphere because the pathway to the surface is blocked by bottlenecks filled with liquid. Thus, the emptying of the pores below the surface may be hindered, and the value of P/P_0 at which a given pore empties is not necessarily determined by its size. By this logic, the adsorption data are more appropriate for conversion to a size distribution. While both arguments make valid points, there remains no consensus as to whether adsorption or desorption data should be preferred.

Another problem with the Kelvin equation analysis is that the distributions calculated by the PV and TV methods are different. The two methods of data collection should be thermodynamically equivalent, but in practice, different adsorption/desorption pathways may be followed, as for the MSQ material in this study. In contrast, all data sets for the SANS porosimetry appear to lie approximately on the same curve (Figure 8), regardless of whether adsorption or desorption data are considered or how data was collected. It is not yet known whether porosimetry data for all materials would lie on such a universal curve or if this phenomenon was unique to the MSQ dielectric in this study. However, at least for this material, the SANS size analysis did not suffer from the same ambiguity that clouds the Kelvin equation analysis.

(26) Everett, D. H. In *Characterization of Porous Solids*; Gregg, S. J., Sing, K. S. W., Stoeckli, H. F., Eds.; London Society of Chemical Industry: London, 1979; p 229.

Summary

Capillary porosimetry experiments combined with in situ SANS measurements reveal quantitative information about pore size and the pore filling process in nanoporous thin films. SANS porosimetry is conducted with a "contrast match" solvent mixture that fills all accessible pores via capillary condensation. The method is most applicable to materials with a homogeneous matrix atomic composition. SANS measurements provide a more quantitative and less ambiguous approach to PSD compared to analysis of adsorption data by the Kelvin equation.

Acknowledgment. We thank International SEMATECH for providing the samples and for financial support and the Office for Microelectronics Programs at the National Institute of Standards and Technology for financial support. We acknowledge the support of the National Institute of Standards and Technology, U.S. Department of Commerce, in providing the neutron research facilities used in this work, and thank Derek Ho and Charles Glinka (NCNR) for maintaining the 8 m SANS equipment. R.C.H. acknowledges the support of a National Research Council/NIST postdoctoral fellowship.

LA036334U